# Validation of the Bayesian sensory uncertainty model of motor adaptation with a remote experimental paradigm

Megan C. Shyr
Mechanical and Aerospace Engineering
University of California, Davis
Davis, CA
mcshyr@ucdavis.edu

Sanjay S. Joshi Mechanical and Aerospace Engineering University of California, Davis Davis, CA maejoshi@ucdavis.edu

Abstract— Understanding human motor learning and adaptation processes is an integral step in developing rehabilitative engineering solutions and training strategies for assistive technologies. Natural skill acquisition enables continually precise movements despite inherent noise in motor execution, sensory perception, and dynamic changes in body parameters (growth, age, etc.) and the external environment. As an initial step, motor learning research has aimed to identify the mechanisms of natural human adaptation during the acquisition of motor skills. Results presented here confirm previous work on motor adaptation using a remote web-based experimental paradigm that could provide a valuable option to conduct additional future work with expanded more diverse subject populations.

Keywords—motor adaptation, prostheses, remote human-subject experiments, assistive technology, human-machine coordination

### I. INTRODUCTION

Humans learn motor skills through both a strategic and adaptive process where strategic processes are sensitive to goal-based performance and adaptive processes are sensitive to prediction errors between the desired and actual outcome of a task [1]. Motor learning research [2]–[4] indicates that during motor skill acquisition humans become highly proficient at estimating and adjusting to the consequences of their movements by creating and storing task-based *internal models* of specific motor skills.

The idea of an internal model is compelling because humans seem to have an uncanny ability to produce precise movements despite inherently noisy motor commands, noisy and delayed sensory feedback, and an unpredictable external environment. Additionally, the human body itself is constantly growing, aging, and dealing with fluctuations brought on by disease, exercise, and mental state – thus indicating some adaptive property of the internal model. Interestingly, transcranial direct current stimulus of the cerebellum has been shown to increase the rate at which subjects adapt in response to fluctuations [4] contributing to the idea that motor adaptation drives internal model calibration. The mechanism for how this is done has become a major focus of research and researchers have long postulated that internal models are maintained through adaptive

processes in response to sensory prediction errors. Bayesian models successfully describe this phenomenon and have been validated in many experimental studies including research on eye saccades [5] and hand reaching [6]–[10].

Existing literature additionally suggests that relevant visual and proprioceptive feedback in movement generation could bolster the adaptation process for rehabilitative applications [9], and the adaptation process can be artificially modulated in taskrelevant dimensions [11]. Moreover, preliminary work in our lab demonstrates evidence for Bayesian motor adaptation behavior in an electromyography (EMG)-based cursor-to-target task, showing potential for application to EMG-driven prostheses [12]. Thus, training strategies capitalizing on innate motor adaptation processes could combat challenges in prosthetic operation including internal changes such as muscle fatigue or external changes such as electrode shift by increasing the rate users adapt to changing task parameters. Other areas of application include human-machine coordination tasks such as supernumerary robotic operation [13]. Shenoy and Carmena have indicated a similar need in brain-computer interfaces in which they argue that neural adaptations are necessary to attain clinically viable levels of performance, and that the development of decoders (or gesture classification systems) alone is not sufficient [1]. They also emphasize that the most effective method of gaining prosthetic and motor skill is to find a way to train users that mimics natural skill acquisition.

Two interesting implications for motor adaptation arise from Bayesian models of visuomotor tasks [9]. Following a Kalman filter (KF) model [14], the first implication is that feedback uncertainty (measurement feedback uncertainty in KF theory) increases trust in the internal model (thus decreasing reliance on sensory feedback) and *decreases* adaptation rate. For example, consider an individual learning to play tennis as dusk sets in. Any changes in ball velocity would theoretically result in limited adaptation as feedback uncertainty increases with the sky darkening. Alternatively, the second implication claims that model uncertainty (model prediction uncertainty in KF theory) decreases trust in the internal model (thus increasing reliance on sensory feedback) and *increases* adaptation rate. For example, a tennis player warming up might be less confident in her internal

model of the task and adapt quickly to any unexpected inaccuracies while an inaccuracy observed after a sufficient warmup might be more likely disregarded. Here the source of uncertainty is dictating the adaptation rate by modulating the Kalman gain or the relative weighting of model prediction and measurement feedback (Fig. 1). While a significant body of literature exists supporting this first implication with cursor-to-target experimental paradigms [6]–[10], research for the second implication is comparatively sparse with mixed results [5], [9], [10]. For this second prediction, further validation is necessary to confirm that distrust in the internal model is the driving factor.

A popular paradigm in motor adaptation experiments is hand reaching in response to visual perturbations [6], [8], [9]. These experiments are typically conducted in a controlled laboratory setting supervised by on-site researchers. Here subjects perform cursor-to-target reaches in a horizontal plane while receiving feedback of hand position on a vertical display (Fig. 2.a). An important experimental element is that online (real-time) feedback during the movement is blocked, allowing researchers to add a small amount of shift (or perturbation) to the position reported back to the subject at the end of the reach. Any subsequent adjustments by the subject in response to these perturbations is recorded as the trial-by-trial adaptation rate. This metric is of interest because it sheds light on the rate at which the internal model updates. Sensory uncertainty is often added to probe the effect of sensory uncertainty on adaptation rate by displaying cursor endpoint feedback as a cursor cloud [8] or a distribution of multiple cursors [9].

Strides have been made by Tsay and colleagues to develop a web-based platform utilizing a trackpad for motor learning and motor adaptation research [15]. Traditional studies require elaborate laboratory setups and finely calibrated hardware to measure movement kinematics. Additionally, these studies are often time intensive as on-site researchers must proctor and administer experimental protocols one subject at a time. Tsay et al. developed an open-source, remote experimental platform (OnPoint) for motor learning studies and demonstrated the capability of web-based systems to closely reproduce results from motor experiments conducted in person [15]. They conducted three visuomotor rotation adaptation experiments in which they evaluated adaptation behavior when hand position was perturbed by angular rotation. Their work confirmed that learning behavior scales with rotation size when both implicit

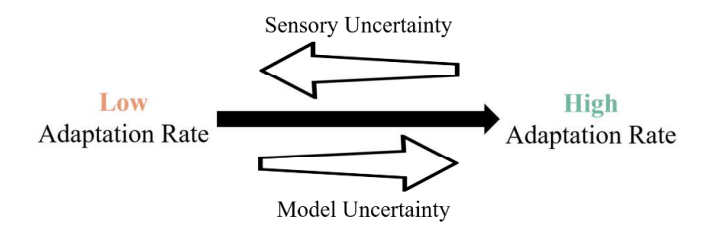


Fig. 1. The Kalman filter gain quantifies the ratio between model uncertainty and sensory uncertainty in Bayesian motor adaptation models. Here arrow directionality signifies an increase in the indicated quantity. As sensory uncertainty increases (toward the left), the adaptation rate decreases, and as model uncertainty increases (toward the right) the adaptation rate increases. Researchers postulate that the brain is performing a similar weighting process when streamlining motor task performance [6].

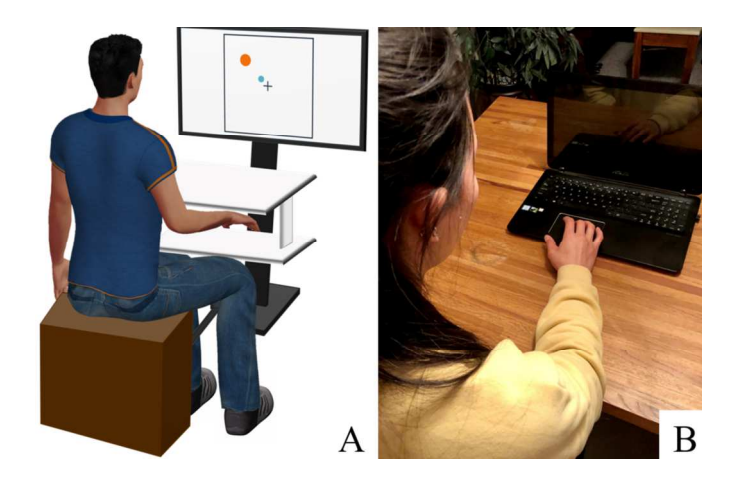


Fig. 2. A depiction of A) a traditional cursor-to-target experimental paradigm, and B) the setup of our analagous remote, web-based experimental paradigm.

and explicit adaptation processes are involved [16], implicit adaptation is invariant to error size [17], and the trial-by-trial adaptation rate function is quasi-linear for smaller rotation sizes but becomes sub-linear for larger rotation sizes [9].

Our work focuses on evaluating the effect of sensory uncertainty on motor adaptation rate with the aim of validating the use of our remote, web-based experimental paradigm. Fig. 2.b. depicts our analogous remote experimental setup. Following methodology outlined by Wei & Körding, we hypothesize that our results will confirm their results [9] by showing that increased sensory uncertainty decreases the trialby-trial adaptation rate in response to visuomotor perturbations. Subject populations are more likely to represent the general population when sourced from web-based platforms [18]. Therefore, an effective remote experimental paradigm could be vital for broadening the homogeneous populations common in scientific research [19]. Furthermore, an effective remote experimental paradigm could be important for continuing motor learning research in challenging circumstances (such as a global pandemic). Lastly, it also enables fast, low-cost turnaround for explorative studies to examine optimal feedback mechanisms and methods to artificially modulate adaptation rate with the overall aim of boosting human-machine cooperation.

# II. METHODS

Eighteen subjects with no history of neurological disorders participated in the experiment (15 female;  $19.8 \pm 1.5$  years old). Seventeen subjects were right-hand dominant, and all subjects had 20/20 vision or corrected to 20/20 vision. Subjects were informed of and consented to procedures approved by the Institutional Review Board at the University of California, Davis (protocol #1677528-2).

# A. Remote Experimental Paradigm

A central aim of this work was to validate the use of a remote, web-based experimental paradigm for motor adaptation studies. A remote platform adapted from [15] was developed in JavaScript/CSS/HTML and deployed through a server managed by the JATOS tool [20]. Subjects completed a cursor-to-target task by performing 'swiping' movements, or reaches, on a laptop trackpad. Key additions to [15] included an automatic

reset of the cursor to the starting point at the conclusion of each trial (reducing additional visual and proprioceptive feedback during the return process), gamification and built-in timeouts to encourage compliance, and the capability to display cursor feedback as a collection of normally distributed cursors. The cursor was a smiley face, the start position was an Earth icon, and the target was an asteroid icon (Fig. 3). Short instruction prompts preceded each block of trials. Attention checks were implemented between blocks and required subjects to comprehend the instructions and click on the correct icon to advance through the experiment. Subjects could time out of the experiment if they were idle for more than 30 seconds (s) during the experimental trials (a 10-s warning was provided after 20 s of no activity). A 'Trial Counter' tracked subject progress through each block as a proportion of trials completed to total trials remaining and 'study progress' tracked overall progress throughout the experiment as a percentage.

# B. Experimental Setup

Prior to the start of the experiment, subjects viewed an instructional video to orient themselves to the task and to learn the appropriate setup. They were instructed to select a flat surface to work, free of obstructions, where they could sit directly in front of their laptop. Additionally, they needed to ensure that they had good wrist support, full access to the trackpad surface, and only used their dominant hand throughout the entirety of the task. Visual examples were shown to demonstrate good and bad setups. Fig. 2.b. shows an appropriate setup. Subjects then viewed examples of successful reaches and the several potential feedback representations or messages they could see during the experiment on the user interface (e.g., endpoint feedback of cursor position with sensory uncertainty, movement speed warnings, etc.). They were reminded to avoid looking down at their trackpad during trials and to focus their

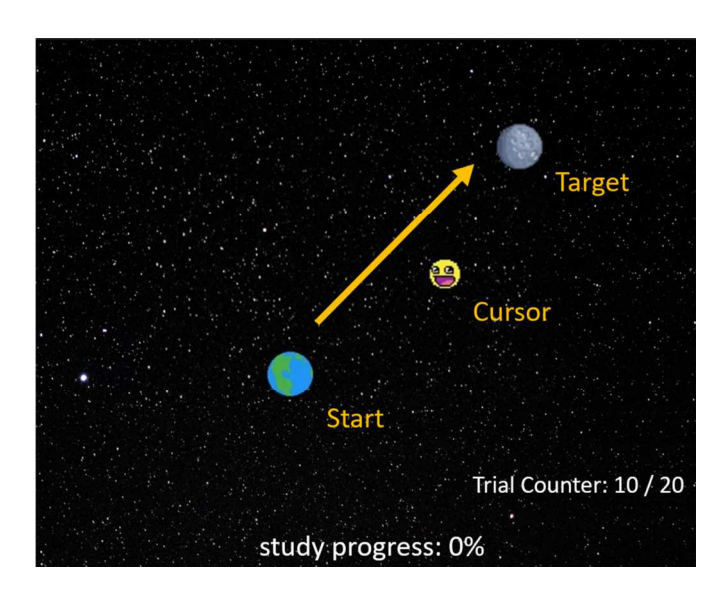


Fig. 3. User interface for the cursor-to-target task. The Earth icon represents the starting point. Prior to each trial, the cursor (smiley face) resets to Earth, and subjects perform 'swiping' movements on their laptop trackpads to hit the target (asteroid) as quickly and accurately as possible. A 'Trial Counter' tracks subject progress through each block of trials. A 'study progress' indicator tracks overall progress through the experiment as a percentage. Note figure is drawn for clarity and is not to scale.

attention on the screen. This reminder was repeated periodically throughout the experimental blocks as well.

Subjects viewed a computer screen with the start directly in the center of the screen. The target distance was set to 300 pixels (px). The start radius, target radius, and cursor radius were scaled according to the target distance resulting in radii of 42.1875 px, 42.1875 px, and 33.75 px, respectively. To successfully complete a reach, subjects had to finish their movement between 30 and 90 milliseconds (ms). Enforcing this range ensured that movement time would not be a significant factor when conducting analysis and confirmed that subjects were not moving slow enough to incorporate visual feedback mid-reach [21]. Subjects were not required to stop on the target, but simply pass through it, and feedback was provided at the point the subject crossed the target distance boundary. After each trial, the cursor was automatically reset to the start. When both the cursor and target appeared, the next reach could be initiated.

# C. Experimental Tasks

Each subject completed an adaptation protocol following [9] in which a perturbation was applied prior to providing cursor feedback to the subject. As a result, trial-by-trial adaptation rate could be quantified by the relationship between change in hand angle of trial k+1 with respects to trial k in response to the perturbation in trial k.

The three phases of the experiment were executed as follows: 1) Familiarization + Condition 1, 2) Washout, and 3) Condition 2 (Fig. 4). Familiarization was the same for all subjects and oriented the subjects to the user interface and required movement. Condition 1 and Condition 2 varied only in the amount of sensory uncertainty provided in the feedback and allowed a within-subject comparison of the effect of sensory uncertainty on adaptation rate. The order of sensory uncertainty level (low or high) for Conditions 1 and 2 was counterbalanced between subjects. See the *Condition 1 & 2* description below for more details.

# 1) Familiarization

All subjects completed a Familiarization block so that they could practice the 'swiping' motion and ensure that they could complete reaches within the required timeframe. Subjects completed 50 trials to a 45° target (+x axis at 0°, following a positive counterclockwise rotation convention). Once the cursor left the start, it was hidden from view. After the cursor crossed the target distance boundary, subjects received a 'Trial Complete!' message. The left-handed subject followed the same protocol but saw a target position at 135° to mirror the wrist movement right-handed subjects used to perform reaches.

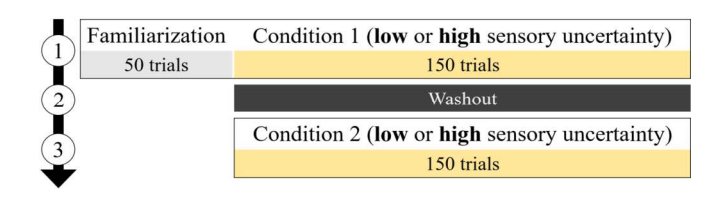


Fig. 4. A within-subject experimental design was utilized to compare the effect of low and high sensory uncertainty on trial-by-trial adaptation rate. The order of sensory uncertainty was counterbalanced between subjects.

# 2) Condition 1 & 2

Both Condition blocks consisted of 50 trials at each perturbation level {-15°, 0°, 15°} in a randomized order for a total of 150 trials. Again, the target was set to 45° (or 135° for the left-handed subject), however, feedback was displayed as a distribution of five cursors to impart a quantifiable amount of sensory uncertainty. Each cursor was displaced following a normal distribution about the position of the hand angle that the cursor crossed the target distance boundary plus the relevant perturbation. Each Condition block varied only in the spread of the cursors (Fig. 5). Moving forward, these two levels will be referred to as low sensory uncertainty and high sensory uncertainty for the smaller distribution of cursors and the larger distribution of cursors, respectively. Fig. 5 shows an example of the two sensory uncertainty levels for a perturbation of 15°. The order of sensory uncertainty level provided (low or high) was counterbalanced across subjects.

The distribution size of cursors for low sensory uncertainty corresponded to a distribution for which 95% of cursor locations were within 1/3 of the perturbation size or  $\pm 5^{\circ}$ . This corresponded to a standard deviation of  $\sqrt{170}$  px. The distribution size for high sensory uncertainty corresponded to a distribution in which 80% of cursor locations were within the perturbation size ( $\pm 15^{\circ}$ ). This corresponded to a standard deviation of  $\sqrt{2726}$  px and was selected such that the perturbations were still perceivable and trial-by-trial adaptation could still occur.

# 3) Washout

Separating the two Condition blocks was a washout task. The purpose of the washout task was to reduce the impact of Condition 1 on Condition 2. This task employed the keyboard arrows as the input to prevent any additional cursor movement calibration outside the Condition blocks. The task was selected out of convenience using existing infrastructure. In this task, the subject's cursor acted as a spotlight that would light up portions of a grid. The task required subjects to utilize velocity control to effectively direct the spotlight around the grid to count the number of circles with orange centers (targets) before the trial

time expired. Subjects were then asked to report the number of targets they located. Lastly, they were provided a score based on accuracy. All subjects completed a short training on the task followed by three trials of the grid search. Note that the washout trials were not analyzed and were completed only to create an interlude between Condition blocks.

# D. Analysis

Subjects who were unable to complete 90% (135/150 trials) of trials successfully during both Conditions 1 and 2 were eliminated from the analysis as any extended length of time between trials may have affected the accurate quantification of trial-by-trial adaptation rate and/or indicate noncompliance. Of the 18 subjects who completed the experimental protocol, three did not meet this standard. As a result, our final analysis consisted of 15 subjects (12 female; 1 left-hand dominant). The inclusion of the left-handed subject did not alter the significance of our results.

Equations (1), (2), and (3) provide a detailed look at the Kalman filter for a linear discrete-time system with timestep k. Equations (1) and (2) give the model prediction and measurement update steps, respectively, where x is the state (target position) estimation, A is the state matrix, and y is the visual feedback. These steps can alternatively be represented as a single equation (3) where the Kalman gain ( $L_k$ ) minimizes the variance of the state estimate by assigning weights based on the relative trust of model prediction versus measurement feedback [14].

$$\hat{x}_{k|k-1} = A_{k-1}\hat{x}_{k-1|k-1} \tag{1}$$

$$\hat{x}_{k|k} = A_{k-1}\hat{x}_{k-1|k-1} + L_k(y_k - y_{k|k-1})$$
(2)

$$\hat{x}_{k|k} = \hat{x}_{k|k-1} + L_k (y_k - y_{k|k-1})$$
(3)

Rearranging (3) yields  $L_k$  as a function of the change in hand angle to the experimentally applied perturbation (the feedback position with the rotation minus the true cursor position). Thus,

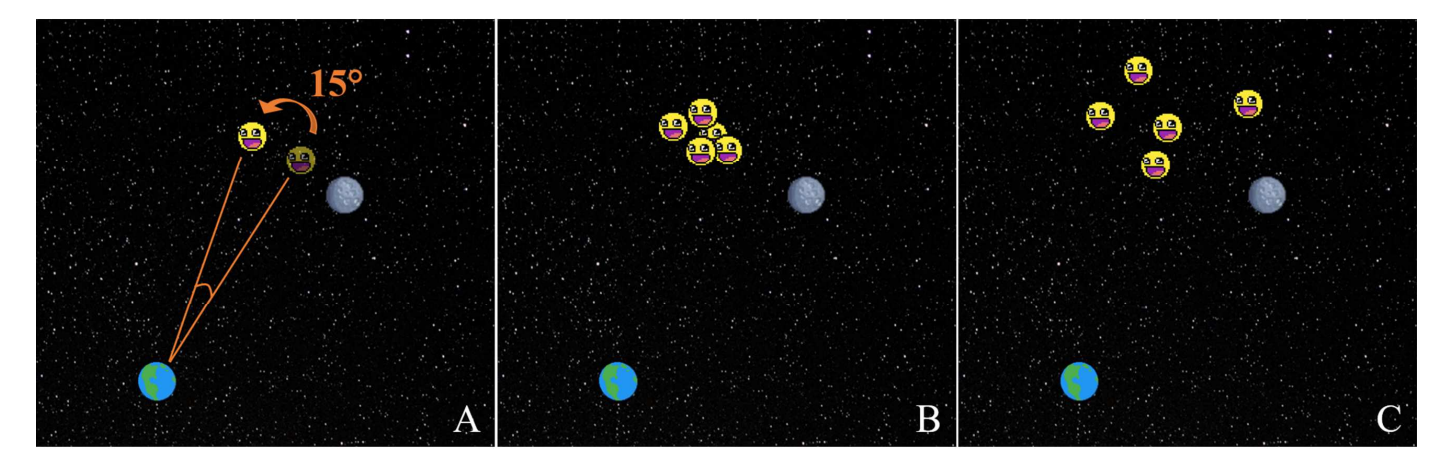


Fig. 5. During Conditions 1 and 2, subjects experienced trial-by-trial perturbations selected randomly from a uniform distribution of  $\{-15^{\circ}, 0^{\circ}, 15^{\circ}\}$ . In A), a +15° perturbation is shown in which the cursor is rotated 15° counterclockwise (unbeknownst by the subject) from the true cursor endpoint (opaque smiley face). Depending on the respective condition, subjects received feedback as either B) a smaller distribution of five cursors (LOW sensory uncertainty,  $\sigma = \sqrt{170}$ ) or C) a larger distribution of five cursors (HIGH sensory uncertainty,  $\sigma = \sqrt{2726}$ ). Each of the five cursor positions were displaced following a normal distribution about the angle that the cursor crosses the target distance boundary plus the relevant perturbation. Note figure not to scale.

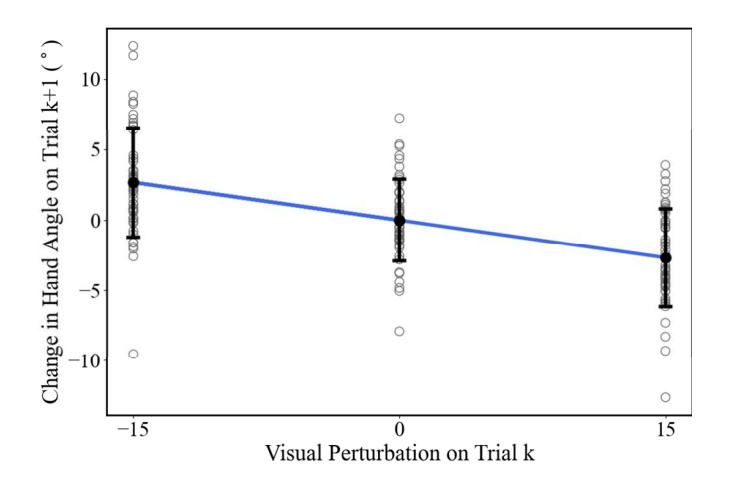


Fig. 6. Trial-by-trial adaptation rate of a representative subject. The gray circles indicate individual trial data, black circles and errorbars are the mean and standard deviations for each perturbation size, and the blue line is the linear regression (adaptation rate). Note that the more negative the adaptation rate, the more proclivity the subject has to adapt to perturbations.

adaptation rate can then be calculated from the linear regression of the change in hand angle to the perturbation from the previous trial [12] (slope in Fig. 6). Two adaptation rates were calculated per subject corresponding to the low and high sensory uncertainty conditions.

# III. RESULTS

Fig. 6 shows a representative subject in which the blue line gives the adaptation rate. Individual trials are plotted (unfilled gray circles) along with the mean and standard deviation of change in hand angle for each respective perturbation level (filled black circles and error bars). Note that the more negative the slope of the line, the more proclivity the subject has to adapt.

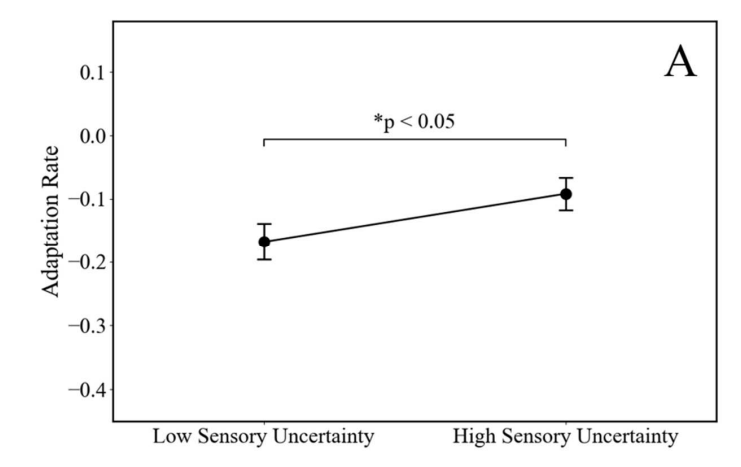
Adaptation rates (mean  $\pm$  standard mean error; sem) across subjects were -0.168  $\pm$  0.029 and -0.096  $\pm$  0.026 for the low sensory uncertainty condition and high sensory uncertainty

condition, respectively (Fig. 7). A pairwise t-test indicated that adaptation rate is significantly different (p < 0.05) and the low sensory uncertainty adaptation rate is significantly more negative (p < 0.01). Thus, human subject data shows that feedback uncertainty slows the rate of adaptation following the Kalman filter model. These results support motor adaptation theory that increased inability to accurately perceive motor consequences encourages subjects to rely more on their internal models, slowing any subsequent internal model updates.

# IV. DISCUSSION

Our reported adaptation rates across subjects (mean  $\pm$  sem) for the low sensory uncertainty and high sensory uncertainty conditions, respectively, are:  $-0.168 \pm 0.029$  and  $-0.096 \pm 0.026$ . Wei and Körding (2010) also verified the first implication of the Bayesian framework by showing that increasing sensory uncertainty decreased trial-by-trial adaptation rate. Reported adaptation rates across subjects (mean  $\pm$  sem) for the low sensory uncertainty and high sensory uncertainty conditions, respectively, are as follows:  $-0.178 \pm 0.015$ ,  $-0.133 \pm 0.017$ , also found to be statistically significant [9]. Thus, our results confirm our hypothesis that increased sensory uncertainty will decrease adaptation rate and confirms published data using a remote and web-based experimental paradigm. Additional support for this implication using lab-based experiments is abundant [6]-[10]. Moreover, our work adds to the efforts of [15] by demonstrating the efficacy for the use of a remote platform for motor adaptation research.

A limitation of our study is the homogenous nature of our subject population – recruited primarily through university undergraduate channels. Recent attention has been brought on the need to reduce research bias [22]. Thus, our remote paradigm could allow the use of web-based resources such as Amazon Mechanical Turk (mtruk.com) and Prolific (prolific.co) to diversify the subject population [18]. Another challenge with our remote study is an inability to control the testing environment, and more specifically, prevent the subject from receiving proprioceptive and visual feedback of their own



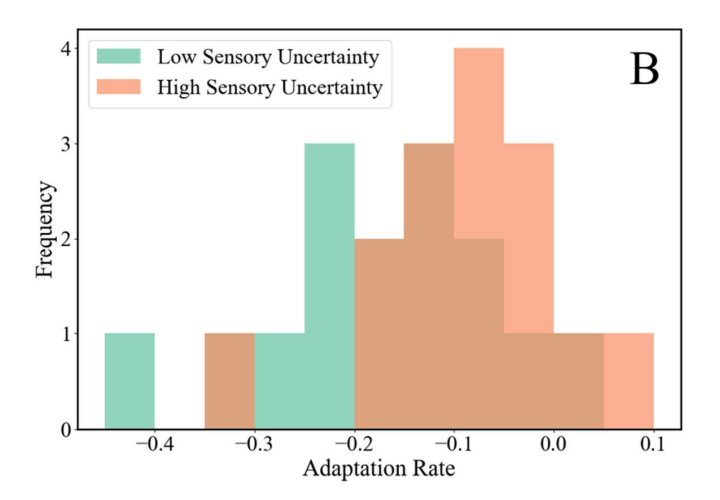


Fig. 7. Adaptation rates (mean  $\pm$  sem) A) were -0.168  $\pm$  0.029 and -0.096  $\pm$  0.026 for the low sensory uncertainty and high sensory uncertainty conditions, respectively. A pairwise t-test indicates that the adaptation rates are significantly different (p < 0.05) and the low sensory uncertainty adaptation rates are significantly more negative (p < 0.01). Results are shown B) for individual subjects as a histogram. Data met the assumption of normality (Shapiro-Wilks) and support the Kalman filter model prediction that increased sensory uncertainty slows the rate of adaptation.

movements. In traditional motor adaptation studies, a platform blocks the subject's hand from view. However, our reaching movement is small and utilizes a trackpad rather than a tablet or robot manipulandum resulting in less informative visual and proprioceptive feedback. We also utilize fast movement times to prevent the effectiveness of any in-motion visual feedback.

Despite these challenges, we propose our work as an initial step to illustrate that careful implementation of a remote study including attention checks, gamification, and built-in timeouts is effective for motor adaptation studies and successful in verifying previously published work. Future work can capitalize on this platform for quick piloting capabilities in the face of limited cost or limited access to in-person testing and continue to move motor learning and motor adaptation research forward. Our next aim is to design experiments, using our remote paradigm, that may help study the second implication of the Bayesian model of motor adaptation that increased model uncertainty leads to increased adaptation rate. This implication is less studied and has mixed results [10], but shows initial promise for application in assistive technologies [12]. Future work will focus on expanding lessons learned to assistive and robotic technologies.

# ACKNOWLEDGMENT

We thank Jason Dekarske for his contribution on the development and the deployment of the remote experimental platform. We thank Kenneth R. Lyons for his invaluable input and mentorship. And lastly, we thank Jonathan S. Tsay and colleagues for providing open-source software upon which we built our platform [15].

### REFERENCES

- K. V. Shenoy and J. M. Carmena, "Combining Decoder Design and Neural Adaptation in Brain-Machine Interfaces," *Neuron*, vol. 84, no. 4, pp. 665–680, Nov. 2014, doi: 10.1016/j.neuron.2014.08.038.
- [2] S. Pasalar, A. V. Roitman, W. K. Durfee, and T. J. Ebner, "Force field effects on cerebellar Purkinje cell discharge with implications for internal models," *Nat Neurosci*, vol. 9, no. 11, pp. 1404–1411, Nov. 2006, doi: 10.1038/nn1783.
- [3] R. C. Miall, L. O. D. Christensen, O. Cain, and J. Stanley, "Disruption of state estimation in the human lateral cerebellum," *PLoS Biol*, vol. 5, no. 11, p. e316, Nov. 2007, doi: 10.1371/journal.pbio.0050316.
- [4] J. M. Galea, A. Vazquez, N. Pasricha, J.-J. Orban de Xivry, and P. Celnik, "Dissociating the Roles of the Cerebellum and Motor Cortex during Adaptive Learning: The Motor Cortex Retains What the Cerebellum Learns," *Cerebral Cortex*, vol. 21, no. 8, pp. 1761–1770, Aug. 2011, doi: 10.1093/cercor/bhq246.
- [5] K. P. Kording, J. B. Tenenbaum, and R. Shadmehr, "The dynamics of memory as a consequence of optimal adaptation to a changing body," *Nature Neuroscience*, vol. 10, no. 6, pp. 779–786, Jun. 2007, doi: 10.1038/nn1901.

- [6] K. P. Körding and D. M. Wolpert, "Bayesian integration in sensorimotor learning," *Nature*, vol. 427, no. 6971, pp. 244–247, Jan. 2004, doi: 10.1038/nature02169.
- [7] M. Berniker and K. Kording, "Estimating the sources of motor errors for adaptation and generalization," *Nature Neuroscience*, vol. 11, no. 12, pp. 1454–1461, Dec. 2008, doi: 10.1038/nn.2229.
- [8] J. Burge, M. O. Ernst, and M. S. Banks, "The statistical determinants of adaptation rate in human reaching," *Journal of Vision*, vol. 8, no. 4, pp. 20–20, Apr. 2008, doi: 10.1167/8.4.20.
- [9] K. Wei and K. P. Körding, "Uncertainty of feedback and state estimation determines the speed of motor adaptation," Front. Comput. Neurosci., vol. 4, 2010, doi: 10.3389/fncom.2010.00011.
- [10] K. He, Y. Liang, F. Abdollahi, M. F. Bittmann, K. Kording, and K. Wei, "The Statistical Determinants of the Speed of Motor Learning," *PLOS Computational Biology*, vol. 12, no. 9, p. e1005023, Sep. 2016, doi: 10.1371/journal.pcbi.1005023.
- [11] H. G. Wu, Y. R. Miyamoto, L. N. G. Castro, B. P. Ölveczky, and M. A. Smith, "Temporal structure of motor variability is dynamically regulated and predicts motor learning ability," *Nature Neuroscience*, vol. 17, no. 2, pp. 312–321, Feb. 2014, doi: 10.1038/nn.3616.
- [12] K. R. Lyons and S. S. Joshi, "Effects of Mapping Uncertainty on Visuomotor Adaptation to Trial-By-Trial Perturbations with Proportional Myoelectric Control," in 2018 40th Annual International Conference of the IEEE Engineering in Medicine and Biology Society (EMBC), Jul. 2018, pp. 5178–5181. doi: 10.1109/EMBC.2018.8513412.
- [13] F. Parietti, "Supernumerary Robotic Limbs (SRL)," MIT d'Arbeloff Lab. http://darbelofflab.mit.edu/robotics-research/supernumerary-robotic-limbs-srl/ (accessed Jun. 15, 2021).
- [14] R. E. Kalman, "A New Approach to Linear Filtering and Prediction Problems," J. Basic Eng, vol. 82, no. 1, pp. 35–45, Mar. 1960, doi: 10.1115/1.3662552.
- [15] J. S. Tsay, A. S. Lee, R. B. Ivry, and G. Avraham, "Moving outside the lab: The viability of conducting sensorimotor learning studies online," bioRxiv, p. 2021.01.30.181370, Feb. 2021, doi: 10.1101/2021.01.30.181370.
- [16] K. M. Bond and J. A. Taylor, "Flexible explicit but rigid implicit learning in a visuomotor adaptation task," *J Neurophysiol*, vol. 113, no. 10, pp. 3836–3849, Jun. 2015, doi: 10.1152/jn.00009.2015.
- [17] J. R. Morehead, J. A. Taylor, D. E. Parvin, and R. B. Ivry, "Characteristics of Implicit Sensorimotor Adaptation Revealed by Taskirrelevant Clamped Feedback," *J Cogn Neurosci*, vol. 29, no. 6, pp. 1061– 1074, Jun. 2017, doi: 10.1162/jocn a 01108.
- [18] G. Paolacci and J. Chandler, "Inside the Turk: Understanding Mechanical Turk as a participant pool," *Current Directions in Psychological Science*, vol. 23, no. 3, pp. 184–188, 2014, doi: 10.1177/0963721414531598.
- [19] J. Henrich, S. J. Heine, and A. Norenzayan, "The weirdest people in the world?," *Behav Brain Sci*, vol. 33, no. 2–3, pp. 61–83; discussion 83-135, Jun. 2010, doi: 10.1017/S0140525X0999152X.
- [20] K. Lange, S. Kühn, and E. Filevich, ""Just Another Tool for Online Studies" (JATOS): An Easy Solution for Setup and Management of Web Servers Supporting Online Studies," *PLOS ONE*, vol. 10, no. 6, p. e0130834, Jun. 2015, doi: 10.1371/journal.pone.0130834.
- [21] H. Z. Zelaznik, B. Hawkins, and L. Kisselburgh, "Rapid visual feedback processing in single-aiming movements," *J Mot Behav*, vol. 15, no. 3, pp. 217–236, Sep. 1983, doi: 10.1080/00222895.1983.10735298.
- [22] A. Howard, C. Zhang, and E. Horvitz, "Addressing bias in machine learning algorithms: A pilot study on emotion recognition for intelligent systems," in 2017 IEEE Workshop on Advanced Robotics and its Social Impacts (ARSO), Mar. 2017, pp. 1–7. doi: 10.1109/ARSO.2017.8025197.